Some Seeding Signatures in Sierra Storms

JOHN D. MARWITZ AND RONALD E. STEWART

Department of Atmospheric Sciences, University of Wyoming, Laramie 82071

(Manuscript received 19 May 1980, in final form 19 June 1981)

ABSTRACT

Airborne seeding experiments were conducted over the Sierra Nevada Mountains in essentially ice-free convective clouds on two days in March 1979 as part of the Sierra Cooperative Pilot Project. On 18 March towering cumuli which extended above a stratiform layer of clouds were seeded, while on 21 March individual towering cumuli were seeded as they developed and moved over the windward side of the mountains. Each cloud was seeded with a vertical curtain oriented perpendicular to the winds during a single pass through the cloud top. The seeding mode was either a low (~0.1 g m^{-1}) or high (~1 g m^{-1}) CO_2 rate or AgI flares (one 20-gram flare per 250 m).

The seeded curtains were penetrated a number of times by the University of Wyoming King Air. The high CO_2 rate apparently overseeded the cloud in that the liquid water was depleted and the cloud dissipated in ~35 min. Even though much of the liquid water was depleted in the other seeded clouds, they persisted and precipitated for over an hour because additional liquid water was condensed through the additional release of convective instability from orographic lifting. The clouds seeded with a low CO_2 rate and with AgI flares yielded similar microphysical characteristics and both methods appeared to have converted the non-precipitating clouds to continuously precipitating clouds.

1. Introduction

A number of long-term operational snow pack augmentation projects have been conducted over the Sierra Nevada Mountains (e.g., Mooney and Lunn, 1968; Elliott and Lang, 1967). Many of these projects began in the 1950's and their objectives were to enhance the snowpack and subsequent streamflow for use in hydroelectric power generation. Analysis of streamflow and precipitation measurements seems to indicate that a 10–15% increase was produced by some of the operations (Advisory Committee on Weather Control, 1957).

The Central Sierra Research (CENSARE) experiment began to provide a much needed physical basis for snow augmentation in the Sierra Nevada. A number of bands were tracked by means of radar across the California Valley and onto the upwind slope of the Sierra Barrier.[1] The bands were oriented almost normal to the wind direction, they consisted of individual cells, and the cells moved with the mean environmental wind direction. From ground observations of the common occurrence of graupel and heavily rimed crystals, Reinking (1975) inferred that regions of significant concentrations of supercooled water were present in Sierra storms and that the accretional growth process was often dominant. Other conclusions from studies in the CENSARE experiment were that the conditions for seedable storms consisted of "warm storms (or storm periods) with deep cloud masses, high [amounts of] moisture, and convective instability from the surface to the −10°C level."[2]

Lamb *et al.* (1976) reported on the liquid water concentration and turbulence encountered over the central Sierra Nevada during a number of aircraft flights by the Desert Research Institute. Within the convective activity, they encountered significant amounts of supercooled water with concentrations of 1–2 g m^{-3} being common near the upwind edge of the convection. The 21 March 1979 case presented here appears to most closely resemble their 22 March 1972 (flight 1) case study.

This study presents some seeding signatures in Sierra storms. The data for the study were obtained from flights on two days in March 1979 during the Sierra Cooperative Pilot Project field season. In the first case study day (21 March), three towering cumulus clouds were each seeded with one curtain of seeding material. The seeding materials were, in order of treatment, a low CO_2 pellet rate (0.1 g m^{-1}), a high CO_2 pellet rate (1 g m^{-1}), and AgI droppable

[1] Peace, R. L., Jr., 1972: Orographic induced circulation observed by radar. *Preprints 15th Radar Meteor. Conf.*, Champaign-Urbana, Amer. Meteor. Soc., 315–320.

[2] Peace, R. L., 1975: The weather modification environment and seed-ability of central Sierra Nevada snowstorms. *Special Regional Weather Modification Conference on Augmentation of Winter Orographic Precipitation in the Western U.S.*, San Francisco, Amer. Meteor., Soc., 79–84.

0021-8952/81/101129-16$08.00
© 1981 American Meteorological Society

Unauthenticated | Downloaded 04/22/24 12:27 AM UTC

flares (one 20-gram flare per 250 m). During the second case study day (18 March) only one convective cloud was seeded and it extended above a stratiform deck. Since ice nuclei were detected on 18 March within the ice crystal plume on most aircraft passes, we correctly concluded that the randomly selected seeding agent was AgI.

The observational systems and operational procedures are described in Section 2. The resulting seeding plumes are discussed in Section 3. Section 4 contains descriptions of and comparisons between the microphysical seeding signatures.

2. Observational systems and procedures

The primary observational system was the Wyoming King Air which was equipped with a full compliment of Particle Measuring Systems probes. These included a Forward Scattering Spectrometer Probe (FSSP) operated in the range of 3–45 μm with 3 μm intervals, an OAP-2D-C in the range of 25–800 μm with 25 μm intervals, an OAP-2D-P in the range 200–6400 μm with 200 μm intervals, an OAP-1D-C in the range 12.5–187.5 μm with 12.5 m intervals. The OAP-2D-C was equipped with depolarization detection. A decelerator also was included in which ice crystals were captured on an oil coated glass slide and stored for later microscopic analysis of ultrafine detail on individual ice crystals. Vertical air motions[3] were computed from measurements made by a vertically stabilized gyro, an accelerometer and a Rosemount angle of attack differential pressure probe. During straight and level flight and for wavelengths <3 km, data from intercomparison flights show that this sytem was capable of measuring vertical velocities consistent with those recorded by the inertial navigation system and gust probe equipped NCAR Queen Air. The King Air data system was computer directed and contained a variety of options for realtime data display. A complete description of the data system and data analysis technique is contained in Cooper (1978).[4]

The King Air was flown repeatedly through a number of different air columns with the aid of position reference subroutines. The subroutines integrated the true airspeed and heading (i.e., dead reckoning) and continuously displayed the magnetic heading and distance from the present position of the aircraft to the air column. As long as the aircraft and air column drifted in the same horizontal winds, the aircraft was in the original air column when the separation distance had decreased to zero. During the experiments on 21 March, we were simultaneously navigating through three separate air columns in sequential order with the aide of the position reference subroutines.

The seeding aircraft was an Aero Commander provided by Aero Systems, Inc. The typical true airspeed for the seeding aircraft was ~80 m s^{-1}. It was equipped with CO_2 hoppers, which dispensed CO_2 pellets at a rate of either 75 g s^{-1} or 7.5 g s^{-1} (1 g m^{-1} and 0.1 g m^{-1}, respectively at normal airspeeds). The aircraft was also equipped with a rack from which flares containing 20 g of AgI could be ejected at variable intervals. The ejection rate used was 0.33 flares s^{-1} (1 flare per 250 m at normal airspeed). Tests made in clear air indicated that the CO_2 pellets fell at least 1 km and that the AgI flares fell ~1 km prior to being consumed. The aircraft's position and seeding events were recorded on digital magnetic tape for later analysis.

a. 21 March 1979 seeding experiment

To conduct the seeding experiments on the convective cells of 21 March 1979 the seeding aircraft pilot and King Air pilot rendezvoused in clear air with the seeding aircraft flying ~0.5 km above and 2–4 km behind the King Air. The King Air was flown near the −12°C level (~3.5 km). The crew in the King Air selected possible convective clouds for seeding near the upwind edge of a wall of towering cumuli located above the 1.2 km topographic contour of the Sierra foothills. During initial penetration of the cloud, the meteorologist (JDM) in the King Air made a final SEED decision if there were significant concentrations of supercooled water (~0.5 g m^{-3}) and no substantial concentrations of natural ice crystals (<5 L^{-1}). If the decision was SEED, the meteorologist in the King Air activated a position reference subroutine on the location of maximum liquid water content in the cloud and instructed the crew of the seeding aircraft to seed with one curtain of material.

The seeding material and rate were usually prescribed by the contents of a sealed envelope which was opened just prior to seeding by the crew onboard the seeding aircraft. On this particular set of experiments the randomized procedure was suspended in order to expedite the experiments. The seeding sequence was prescribed by the meteorologist in the King Air as low CO_2 rate, high CO_2 rate and AgI flares. This sequence was selected because it was thought, based on previous experiments, that the low CO_2 rate would produce a distinctive and probably long-lasting microphysical signature. On the other hand, the high CO_2 rate was expected to produce a dramatic but short-lived seeding signature. The seeding signatures from the AgI flares was not anticipated. Because the expected seeding

[3] Rodi, A., 1979: Air motion sensing with the University of Wyoming aircraft data system. Rep. No. AS 120, Dept. Atmos. Sci., University of Wyoming, 84 pp.

[4] Cooper, W. A., 1978: Cloud physics investigations by the University of Wyoming in HIPLEX 1977. Rep. No. AS 119, Dept. Atmos. Sci., University of Wyoming, 320 pp.

Unauthenticated | Downloaded 04/22/24 12:27 AM UTC

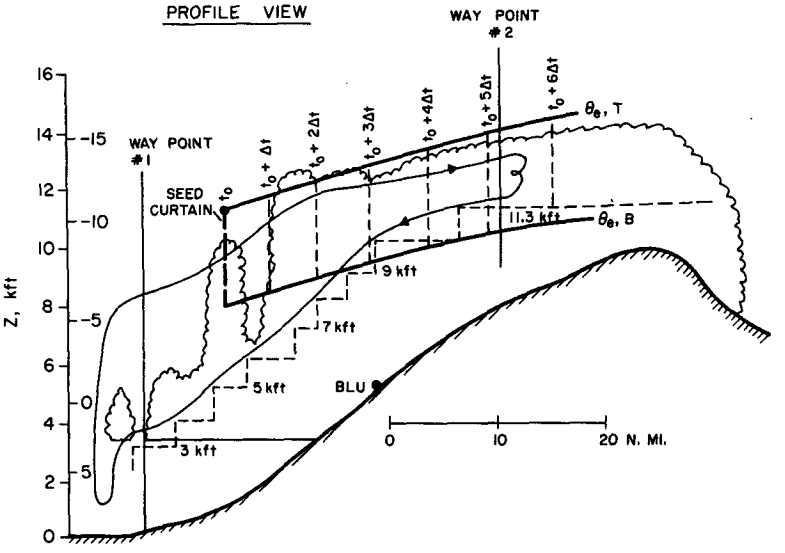

FIG. 1. The dashed stair-step line is the minimum obstruction clearance altitude (MOCA) along I-80 through Blue Canyon (BLU). θ_e, T and θ_e, B are the equivalent potential temperatures at the top and bottom of the seed curtain, respectively.

signatures were observed, all the seeding modes were tested in a short time.

At 15–45 min intervals the seeding aircraft was again rendezvoused with the King Air, another vigorous nearly ice-free towering cumulus was selected near the geographic position of the original test cloud, it was seeded, and then each of the seeded clouds was observed by flying upwind-downwind from one seeded cloud to the next in sequence. Using the position reference subroutines this was not difficult. The downwind passes were generally flown at the higher altitudes, while approximately half of the upwind passes were flown at minimum obstruction clearance altitudes which in practice were ~1 km above the local terrain. The other upwind passes were made at a variety of higher altitudes.

b. 18 March 1979 seeding experiment

The seeding experiment on 18 March 1979 was conducted using the routine presented in schematic form in Fig. 1 which is quite similar to the routine described above and used on the 21 March seeding experiment.

In this experiment the seeding aircraft was not led through the SEED GATE but rather was instructed to seed between two points after the King Air system had determined that supercooled water and a dearth of ice crystals were present. The seeding aircraft then made one pass while seeding with the agent prescribed in a set of randomized envelopes. The crew in the seeding aircraft obviously knew the seeding mode but did not divulge this information to anyone except the field manager and neither participated in the cloud or SEED GATE selection nor assisted in the evaluation of the experiment.

3. Seeding plumes

a. 21 March 1979 seeding experiments

The thermodynamic sounding from the surface to 500 mb during takeoff and climbout over the upwind valley is shown in Fig. 2. The inversion at 875 mb is typical for the California Valley. The convective clouds were initiating over the 1.0–1.5 km contours with cloud bases at ~825 mb (+2°C). The cloud tops were near 600 mb (−15°C) and the maximum θ_e observed in cloud was 304 K, corresponding to a thermal buoyancy of +1°C. The winds were westerly at ~6 m s^{-1} throughout the cloud level.

Fig. 3 is a cloud photograph taken from the King Air ~1 min prior to penetration and seeding with the low CO_2 rate. Note the clear area to the right of the experimental cloud.

Fig. 4 contains analog traces of several parameters from 2333 to 2335 (all times are GMT) while on a downwind (easterly) heading. This pass was made at 3.6 km (−12°C) and corresponded to 3.5 min after the Agl seeding experiment and 23 min after the high CO_2 seeding experiment. The peaks in liquid water[5] (~1.2 g m^{-3}) were associated with the peaks in vertical velocity (4–6 m s^{-1}). The narrow spikes (4 s

[5] Johnson-Williams measured liquid water contents were within 20% of the FSSP derived liquid water contents.

Unauthenticated | Downloaded 04/22/24 12:27 AM UTC

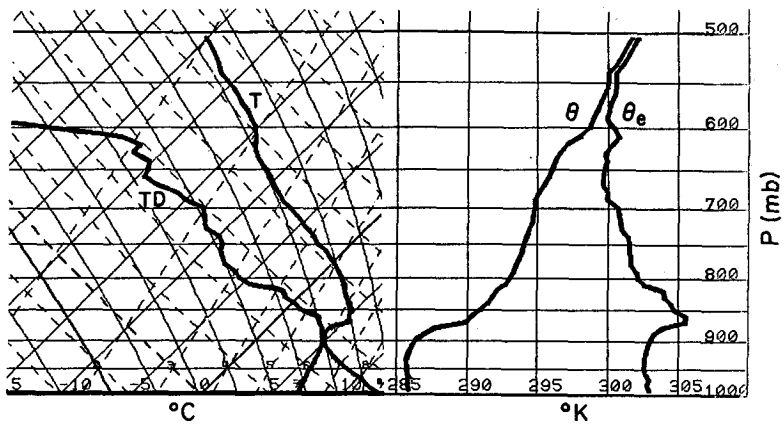

FIG. 2. Sounding on 21 March 1979 during takeoff and climbout. The temperature (T) and dewpoint (TD) are plotted on a skew-T log-p diagram. Potential temperature (θ) and equivalent potential temperature (θ_e) are plotted on the right side of the diagram.

or ~400 m) observed by both the 2D-C and 1D-C instruments were due to ice crystals produced by the AgI flares. The peak concentration of ice crystals as detected by the 1D-C probe was ~2000 L^{-1} while the peak concentration as detected by the 2D-C probe was only ~30 L^{-1}. The difference in concentration was because few crystals had grown to detectable sizes (50 μm) for the 2D-C probe.

The ice crystal plume detected by the 2D-C and 1D-C probes beginning at 233410 was in the cloud seeded with high CO_2 rate 23 min earlier. Note that almost all of the liquid water had been depleted and the 1D-C concentrations had decreased to ~100 L^{-1}. Also note that the vertical velocity variations and magnitudes appear to be less than in the newly seeded cloud.

From the data on the AgI plume, the response characteristics of the NCAR counter to a pulse of ice nuclei can be determined. The first ice crystals in the cloud chamber to be detected by the acoustic counter occurred ~25 s after entering the ice crystal curtain. Since the typical growth rate for ice crystals is ~1 μm s^{-1} and the threshold for particle detection by the acoustic counter is ~25 μm, these times

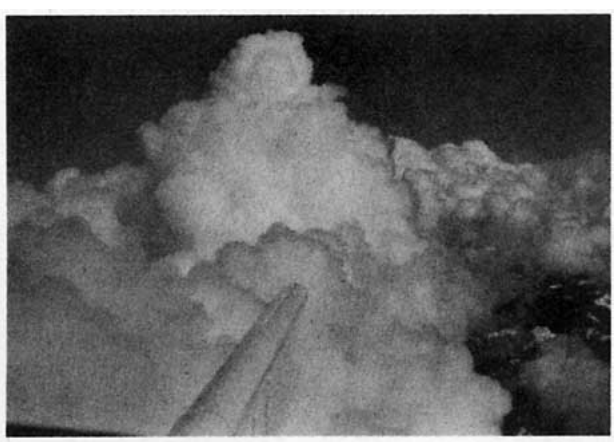

FIG. 3. Cloud photo from King Air at 1 min prior to penetration and seed with low CO_2 rate. Note the nose bottom in the lower foreground.

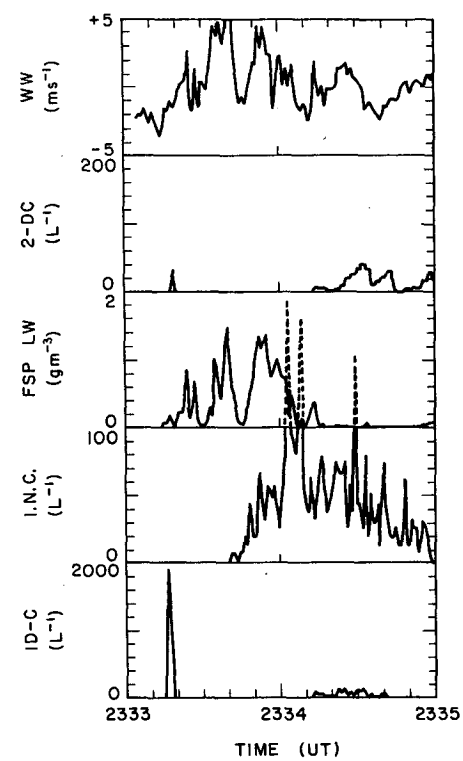

FIG. 4. Analog traces from 2333 to 2335. Vertical velocity (WW) is in m s^{-1}, 2D-C total concentration is in L^{-1}, FSSP liquid water (FSSP-LW) is in g m^{-3}, ice nuclei concentration (INC) is in L^{-1} and 1D-C concentration is in L^{-1}.

Unauthenticated | Downloaded 04/22/24 12:27 AM UTC

are physically consistent. The average peak in ice nuclei concentration (INC) was ~75 L^{-1} and it occurred ~55 s after the curtain was intersected. The concentration of ice nuclei decayed to e^{-1} of the peak value (i.e., ~25 L^{-1}) ~1 min after the peak occurred.

Fig. 5 contains another series of analog traces from the King Air while on a downwind (easterly) heading from 2342 to 2345. The pass was made at 3.5 km (−11°C) which corresponded to 13.5 min after the AgI seeding experiment. The vertical velocities prior to 234310 were recorded during a turn and therefore are not valid. After recovery, the variations and magnitudes of the vertical velocities were qualitatively less than those in the previous penetration shown in Fig. 4. The width of the ice crystal plume was now 28 s or 2800 m, the peak 2D-C concentrations now exceeded 100 L^{-1}, and the 1D-C concentrations had decreased to ~500 L^{-1}. The first ice nuclei appeared ~25 s after the first ice crystals were encountered and the average peak ice nuclei concentrations occurred ~55 s after the peak in ice crystal concentrations.

Probably the most significant feature in Fig. 5 is the liquid water content trace. Even though most of the liquid water was depleted in the region of high ice crystal concentrations, there was a small amount of liquid water present within the ice crystal plume and there was a substantial amount of water in regions surrounding the plume. The obvious explanation is that additional convective elements developed in the immediate vicinity of the seeded cloud. Whether the additional convective elements are a "dynamic seeding effect" and/or simply an orographic effect can only be determined by additional seeding experiments in which natural, nonseeded clouds are examined with the same detail as the seeded clouds.

Fig. 6 contains a 2 min panel of data for each pass through each seeded cloud. The solid lines are analog traces of liquid water content and the dashed lines are analog traces of 2D-C concentrations. The segments through the clouds seeded with the low CO_2 rate, high CO_2 rate and AgI flares are presented in the left, center and right columns, respectively. The segment through the cloud seeded with the low CO_2 rate continues in the middle of the center column. The time with respect to seeding, altitude and temperature is indicated in each panel. From the initial pass (Δt = 0 min) it may be seen that the horizontal width and liquid water contents of the clouds were similar at the −12°C level and that few natural crystals were present. The first passes after seeding (Δt = 3 min) were made on an easterly heading, (i.e., orthogonal to the seeding passes) and indicate that each ice crystal plume resulting from seeding was ~5 s in width and was located on the upwind or western side of each cloud. This was by design because it was thought that the ice crystals

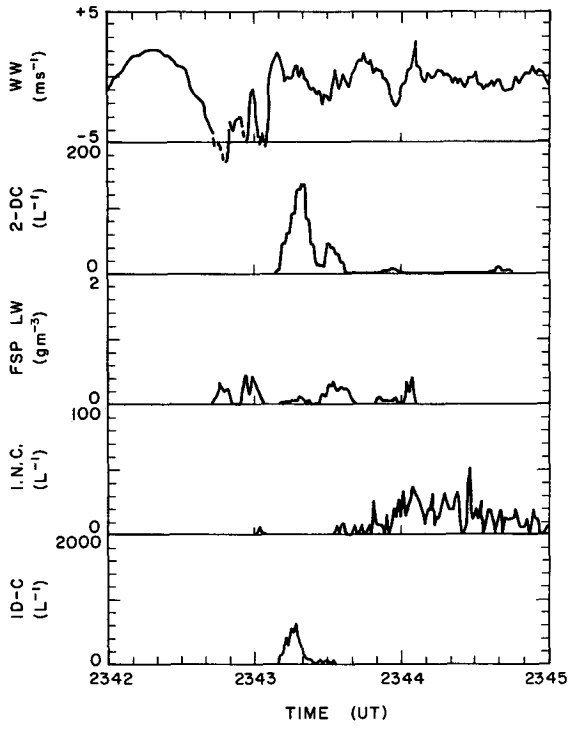

FIG. 5. As Fig. 3.3 except for time period from 2342 to 2345.

produced by seeding would readily spread downwind due to the wind shear. At Δt = 33 min for the cloud seeded with the high CO_2 rate, there was no liquid water present, whereas the other clouds continued to display some regions of liquid water through the period of observations. We continued to penetrate the middle cloud beyond Δt = 33 min but no liquid water or ice crystals were detected. Due to fuel shortage we had to terminate the experiments even though the first and last clouds were still active, vigorous and west of the Sierra crest.

Based on this experiment and a few other experiments, the response of the cloud to the high CO_2 rate was typical. After ~20 min the cloud was totally glaciated such that when inside the plume, blue sky and the ground were clearly visible but many scintillating ice crystals were visually observed.

The plume trajectories for all seeded clouds are shown in Fig. 7. From the available King Air data the lateral boundaries of the plumes and the outlines of the plume at 30 min intervals are shown. The lateral boundaries of the plumes were dashed between Δt = 30 and 60 min for the first cloud because no passes were obtained while initiating the second experiment. It is significant that the geographic locations of each cloud at Δt = 0 were within 5 km of each other (5 km north and 35 km west of the LTA VOR) and that the trajectories overlapped each other. Our visual impressions were that these were individual clouds in a cloud street

Unauthenticated | Downloaded 04/22/24 12:27 AM UTC

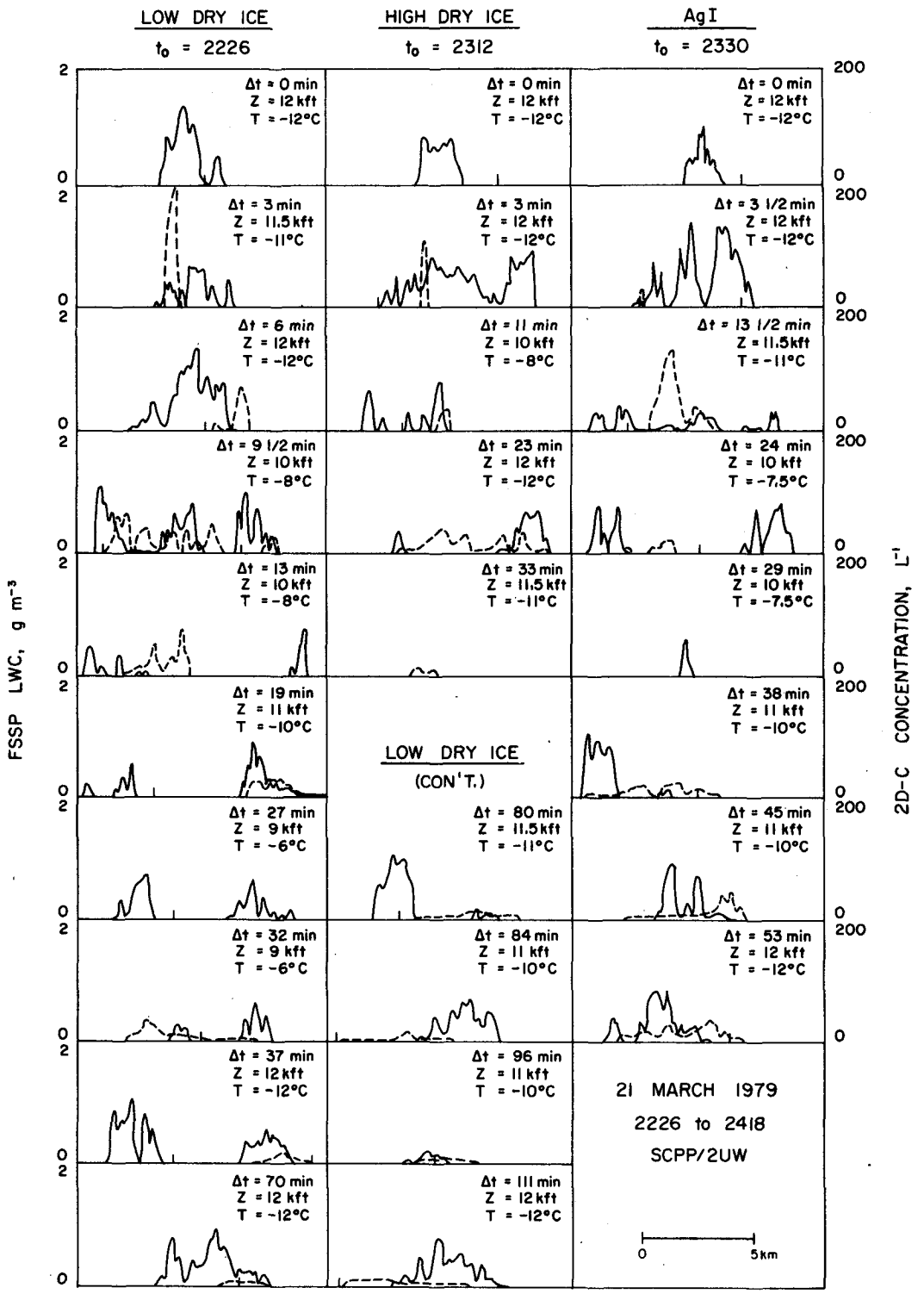

FIG. 6. Composited analog traces for each penetration of a seeded cloud on 21 March. Each panel is 2 min in length and contains a trace of FSSP liquid water (solid line) and a trace of 2D-C concentrations (dashed line). The time of penetration after seeding, altitude and temperature is indicated in each panel.

in which clear areas existed between each cloud of the street as well as between other cloud streets. Because of the clear areas and the lack of vertical wind shear, no indications of microphysical interaction between the clouds in the cloud street were observed.

Unauthenticated | Downloaded 04/22/24 12:27 AM UTC

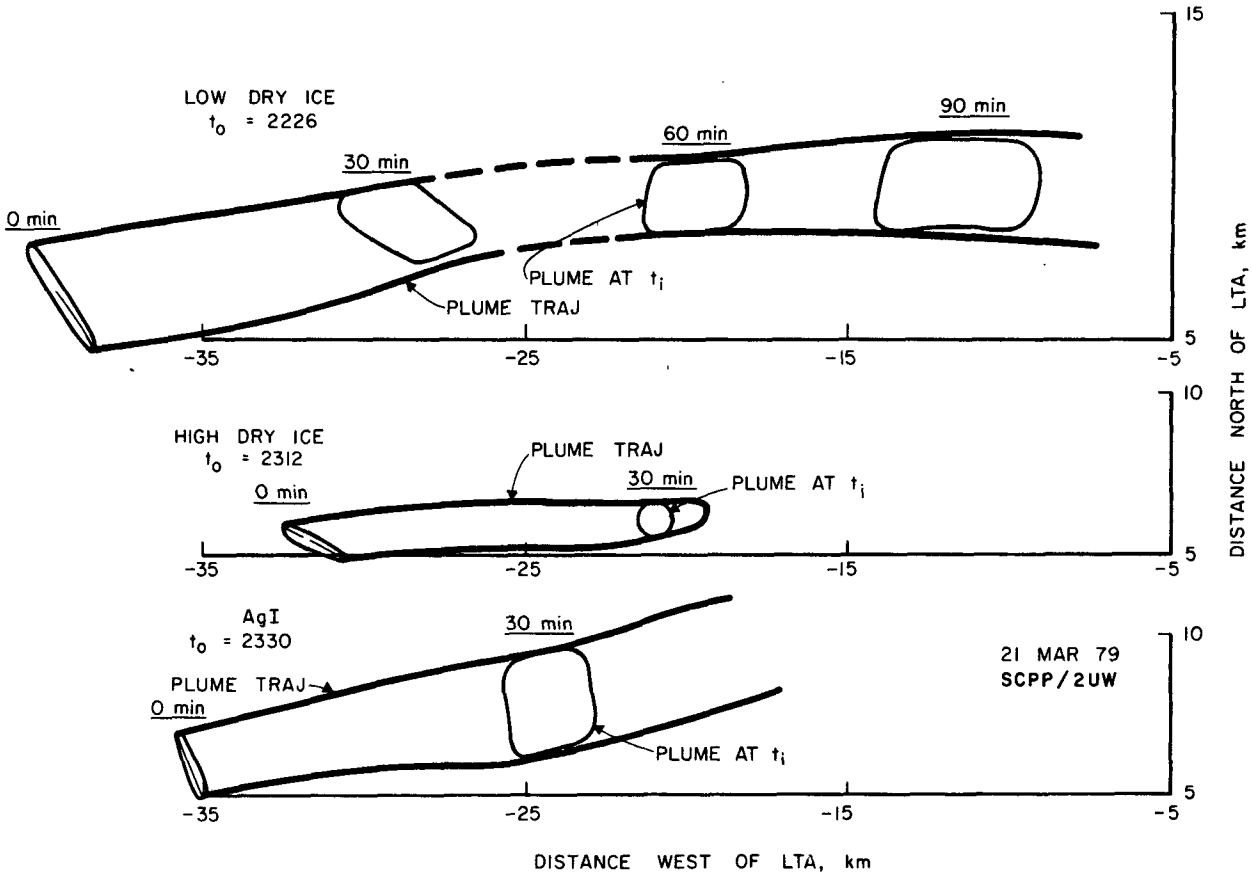

FIG. 7. Plume trajectories (wide line) and plume locations at 30 min intervals (thin line) for each seeded cloud. Lake Tahoe (LTA) VOR is located on the Sierra crest.

The area of the seeded plume as a function of time is plotted in Fig. 8 for each of the clouds. For the first 30 min the area of the plumes for the low CO_2 and AgI were similar, while the area of the plume for the high CO_2 was much less and decreased to zero after ~30 min. No data were available for the AgI plume beyond ~45 min but the area of the low CO_2 plume remained constant between 30 and 60 min and then expanded significantly from 60 to 100 min. Weickmann (1973) reports seeding some Great Lakes storms with 320 kg of CO_2 and with 2.1 kg of AgI. The seeding routine consisted of flying between two way points for periods of 10 to 30 minutes. The seeded areas grew to ~300 km^2 for CO_2 and ~150 km^2 for AgI at 30 min after the first radar echo.

b. 18 March 1979 seeding experiment

The thermodynamic sounding from the surface to 575 mb during descent and landing is shown in Fig. 9. The cloud-base temperature, pressure and θ_e were +1°C, 850 mb and 298 K, respectively. The cloud top photograph (Fig. 10) was taken from the King Air 16 min after seeding while looking to the north. The cloud was stratiform with distinct convective elements extending from the top. The scattered cirrus was not a factor. The winds within the stratiform clouds were from SSE at 6 m s^{-1}, consequently the trajectory of the seeded plume was parallel to the topographic contours.

Fig. 11 contains a series of analog traces from the King Air from 1935 to 1940. This pass was made 18.5 min after seeding at 3.4 km (−11°C) while on a southerly heading. The 1D-C probe recorded particle concentrations of ~1000 L^{-1} in the same region. The width of the ice crystal plume was ~6 km. It is significant that liquid water contents in excess of 2 g m^{-3} were present on the north side of the ice crystal plume, and that liquid water contents of

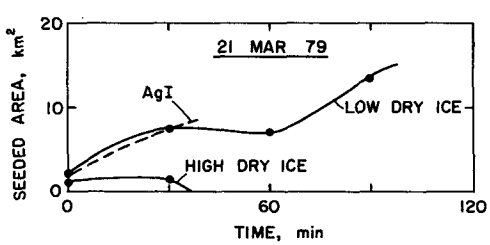

FIG. 8. Seeded area as a function of time for the seeding experiments.

Unauthenticated | Downloaded 04/22/24 12:27 AM UTC

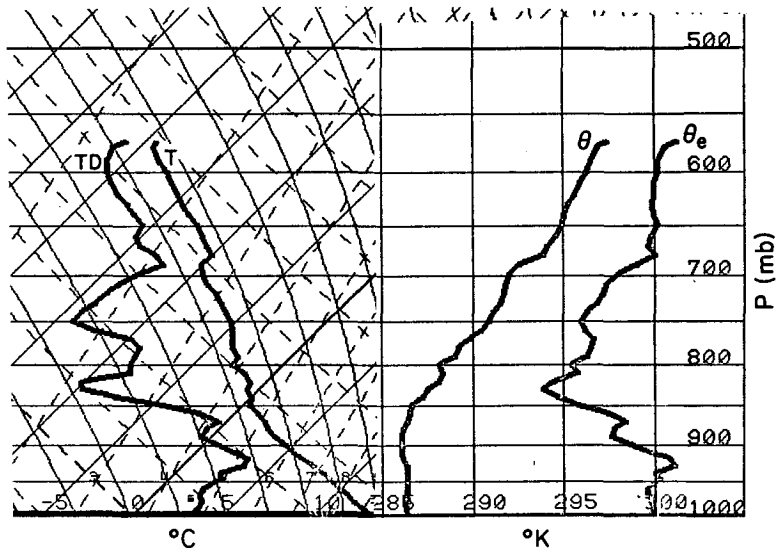

FIG. 9. As in Fig. 2 except for 18 March 1979 during descent and landing.

1 g m^{-3} were observed *within* the ice crystal plume. From the ice nuclei trace it is seen that the first ice nuclei were recorded ~45 s after entering the ice crystal plume and the average peak ice nuclei concentrations were recorded ~70 s after the peak ice crystals were encountered.

Fig. 12 contains a 2 min segment of data for each pass through the cloud seeded with AgI flares. From the pre-seed pass ($\Delta t = -6$ min) and the seeding pass ($\Delta t = 0$) it may be seen that the liquid water region was extensive and that there was no significant concentration of natural ice crystals. The first pass after seeding ($\Delta t = 9$ min) indicates that a large spike of ice crystals was present on the southern edge of the supercooled water cloud with concentrations of ~150 L^{-1}. In addition, it may be noted that natural ice crystals appeared within the supercooled cloud with concentrations of ~10 L^{-1}. The ice crystal plume continued to spread and be tracked for 150 min with apparent regeneration of supercooled water through development of additional convection. It is not known whether the development of additional convection was a natural process or a dynamic response of the seeding.

The trajectory of the ice crystal plume is shown in Fig. 13. From the available penetration data the outlines of the plume at 30 min intervals were also estimated. (Insufficient penetration data were available near 120 min to identify the plume.) The initial speed of the plume was 6 m s^{-1} during the first hour and increased to 7.5 m s^{-1} during the last hour. The lateral dimension of the plume reached a steady state dimension of ~10 km while the longitudinal dimension appeared to continue expanding at the rate of ~2 m s^{-1}.

The area of the seeded plume is plotted as a function of time in Fig. 14. The area expanded at ~1 km^2 min^{-1} for the first 100 min, after which the rate of expansion decreased significantly. Weickmann (1973) reported that the Great Lakes stratocumuli seeded with CO_2 and AgI expanded at about four to five times this rate. Since his observations of plume dimensions were significantly different from these, it is not known how comparable are the results.

FIG. 10. Cloud photo from King Air at 1935 ($\Delta t = 16$ min).

4. Microphysical observations of seeding effects

Fig. 15 shows FSSP droplet spectra prior to seeding for the three clouds which were seeded on March 21. The peak in all spectra occurred ~14–15 μm, and there were only a few droplets as large as 25 μm diameter. Liquid water contents varied between 0.4 and 0.7 g m^{-3}, droplet concentrations

Unauthenticated | Downloaded 04/22/24 12:27 AM UTC

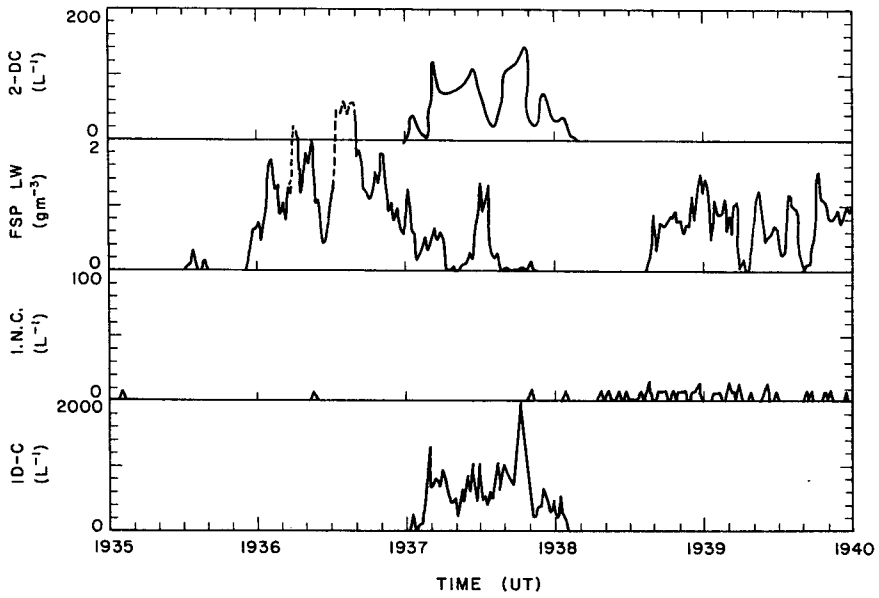

FIG. 11. As in Fig. 4 except for 1935 to 1940 on 18 March. The upper trace is 2D-C depolarized concentrations (2D-1) in L^{-1}.

ranged between 300 and 470 cm^{-3} and mean diameters were between 12 and 13 μm. Based on these microphysical similarities, it would be expected that the clouds would respond in much the same manner to identical seeding treatments. Variations in the evolution of the microphysical characteristics of the clouds should therefore reflect differences attributable to seeding method.

Fig. 16 shows the evolution of the 1D-C size spectra for the three seeding agents. Although the spectra were hand-drawn through plotted data points, the data points were aligned in an extremely linear manner. The exponential distributions may be a consequence of there being only one growth process, namely diffusion, dominating in this size range of particles. The left diagram corresponds to ~3 min after each seeding, and the right diagram corresponds to ~35 min after each seeding. Note that the observational temperatures were $-11°C \pm 1°C$. The spectral characteristics at 3 min after seeding will be discussed first. The intercepts and slopes were dependent upon the seeding method utilized. The highest intercept was associated with the high CO_2 seeding rate, the flattest slope was produced by the low CO_2 rate and the slopes produced by the high CO_2 and AgI were nearly parallel. Even though the high CO_2 rate was an order of magnitude higher than the low CO_2 rate, relative concentrations only differed by a factor of about 6.

Although speculative, one can present qualitative arguments to explain some of the relationships between the slopes. First, consider the relative slopes of the AgI mode and the low CO_2 rate. The low CO_2 rate produced large numbers of particles at a specific time. These particles grew and therefore the number of very small particles decreased as a function of time. For the case of the AgI mode, this chain of events did not occur. Initially, there was a large number of ice crystals produced through nucleation, but there were also particles nucleated at later times. In other words, small particles were produced over a longer period of time. In comparing the two agents, it would be expected that the AgI mode would show a higher relative number of small particles as compared to larger ones. This means that, as observed, the AgI mode would produce size spectrum characterized by a steeper slope than that resulting from CO_2 seeding. Second, consider the relative slopes between the high CO_2 rate and the low CO_2 rate. There were many more particles produced by the high CO_2 rate than by the low CO_2 rate. It may be that the larger number of particles produced by the high CO_2 rate reduced the water vapor amounts to low values over larger portions of the plume than was the case for the low CO_2 rate. Because of this, more of the particles produced by the high CO_2 rate would not be able to grow or would grow more slowly. As a result, the slopes, as observed, would be steeper for the high CO_2 case than for the low CO_2 case. Although these arguments are speculative and qualitative, they do explain the observations.

The right diagram in Fig. 16 shows the 1D-C size spectra approximately 35 min after seeding. The slope associated with seeding by the high CO_2 rate

Unauthenticated | Downloaded 04/22/24 12:27 AM UTC

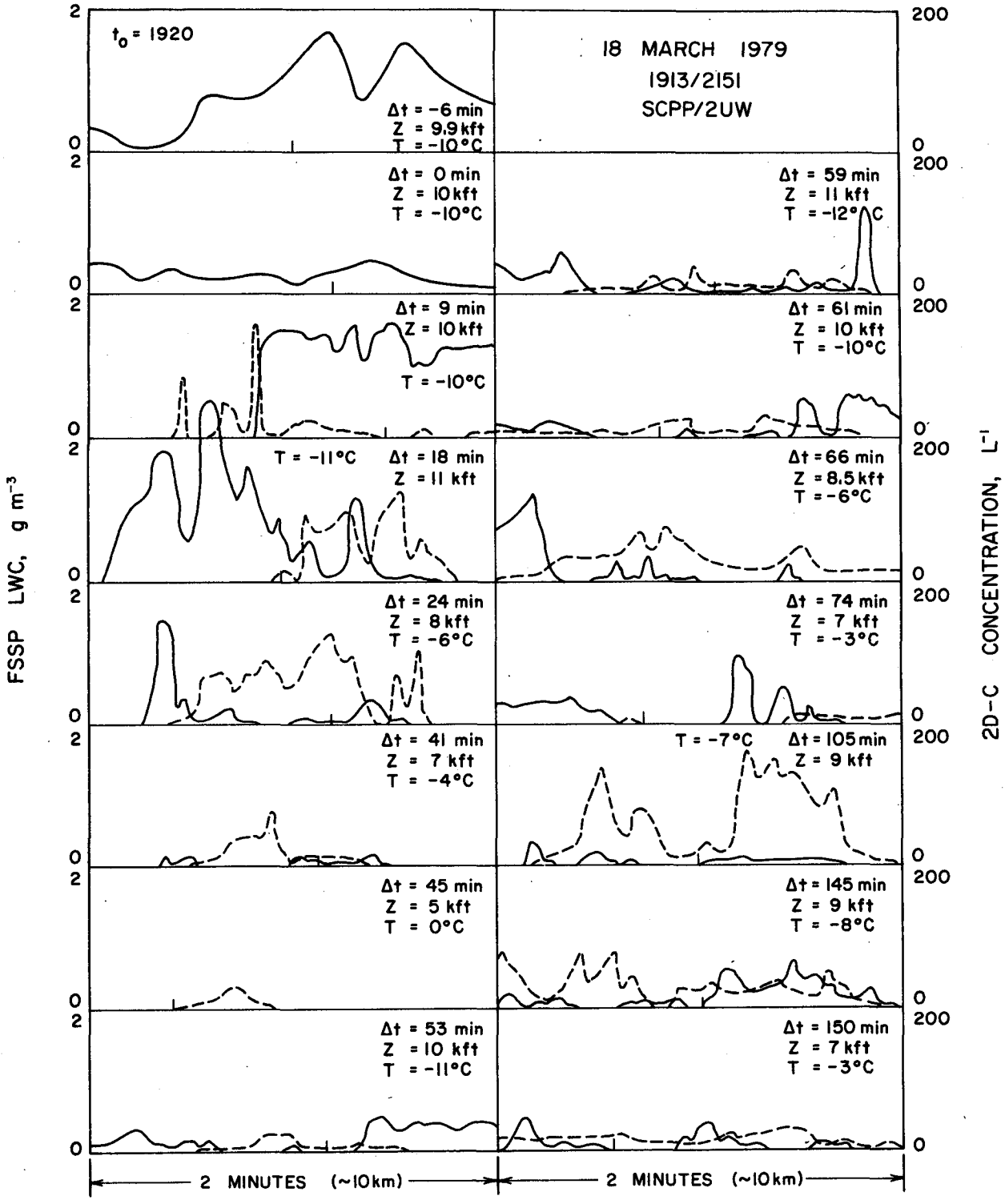

FIG. 12. As in Fig. 6 except for 18 March.

was essentially the same as it had been after 3 min, but the intercept was less by two to three orders of magnitude. The later time corresponds to the last pass which was made through this cloud and suggests that the cloud was in its dying stage. The slopes of the other two spectra were even steeper than the

Unauthenticated | Downloaded 04/22/24 12:27 AM UTC

high CO_2 case and these cases were characteristic of clouds that continued to exist for long periods after 35 min. For the low CO_2 and the AgI case, the intercepts at 35 min were less than an order of magnitude lower than what they were at 3 min, so that a mechanism must have been operating in these clouds by which new crystals were continually being generated.

Fig. 17 shows the particle evolution associated with seeding by the low CO_2 rate; this progression was typical for the other seeding modes as well. Times of cloud penetration were 3, 9.5, 19, 37 and 111 min after seeding. Sizes increased from very small (300 μm) to quite large (>1 mm). Initial particles at 3 min, as determined from ice crystal slides, were mainly plates that either had a little rime or were pristine. On the ice crystal slide, there was also one heavily rimed column. By 9.5 min particles of up to 400 μm existed, by 19 min the largest particles were of the order of 1 mm, and at 37 and 111 min, some particles were well in excess of 1 mm. From 9.5 to 37 min, the particles appeared to be heavily rimed graupel-like particles, but by 111 min they appeared to be less heavily rimed and more aggregate-like.

Figs. 18–20 and Table 1 show the evolution with

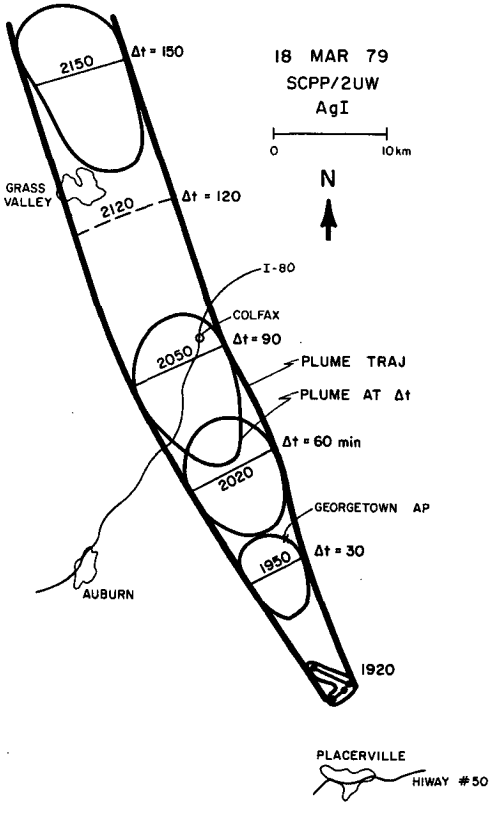

FIG. 13. As in Fig. 7 except for 18 March.

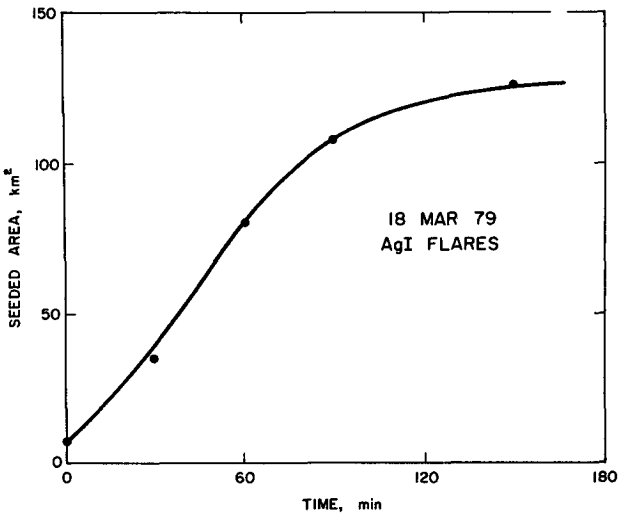

FIG. 14. As in Fig. 8 except for 18 March.

time of the 2D-C size spectra for each of the three different seeding agents: low CO_2 rate, AgI mode, and high CO_2 rate. The results shown in these figures are means across the detectable plume width. The seeding agents produced some similar features as well as, in some cases, distinct differences.

Fig. 18 shows the particle characteristics attributable to the low CO_2 rate. There are several aspects of the results that can be discussed. First, there was a general evolution toward larger sizes with time. At 3 min, the largest particle size was ~300 μm; at 9.5, ~0.7 mm; and at 19, 37 and 111 min, the largest particles were >1.5 mm. Second, although sample volume uncertainties may have influenced the shape of the spectra at small sizes, there appeared to be a strong peak in the distribution through 19 min and associated spectral distributions were *not* exponential distributions. At 3 and 9.5 min the peak occurred near 150–200 μm, by 19 min the peak was less abrupt but the slope was much flatter at small sizes, and by 37 min the distribution had become exponential so that there was no indication of the initial peak in the size distribution at the small sizes. Third, between 37 and 111 min, microphysical size distributions changed very little. Fourth, the largest concentrations of small crystals (<500 μm) were encountered during the penetration at 9.5 and 19 min after seeding.

Fig. 19 illustrates the 2D-C size spectra for the AgI case. There are several features which can be discussed. First, there was a continual increase in maximum particle size so that by 53 min there were substantial concentrations ($>10^{-3}$ L^{-1} μm^{-1}) of particles at large as 1.5 mm. Second, there was a peak in the size distributions near 150 μm at 3.5 min. The peak was at 300 μm by ~13.5 min but by 53 min there was no longer a peak and the distribution

Unauthenticated | Downloaded 04/22/24 12:27 AM UTC

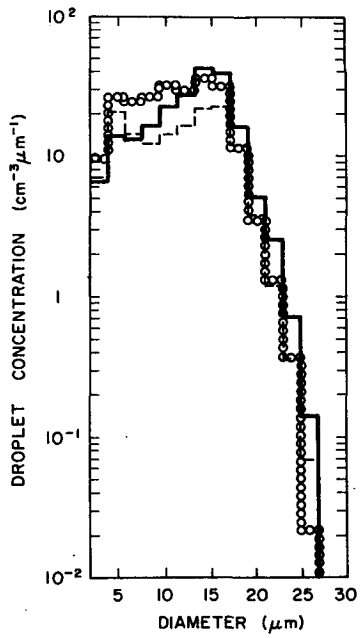

INITIAL LIQUID WATER CHARACTERISTICS ON MARCH 21, 1979

AGENT	LIQUID WATER (g m^{-3})	DROPLET CONC. (cm^{-3})	MEAN DIAMETER (μm)
LOW CO_2	0.7	413	13.3
AgI	0.4	300	12.0
HIGH CO_2	0.6	470	11.6

FIG. 15. Average cloud droplet spectra obtained in the clouds seeded on 21 March, 1979 prior to the seeding events. Spectra from the three clouds seeded with low CO_2 rate, AgI, and high CO_2 are indicated on the diagram.

EVOLUTION OF 1D-C SIZE SPECTRA ON MARCH 21, 1979

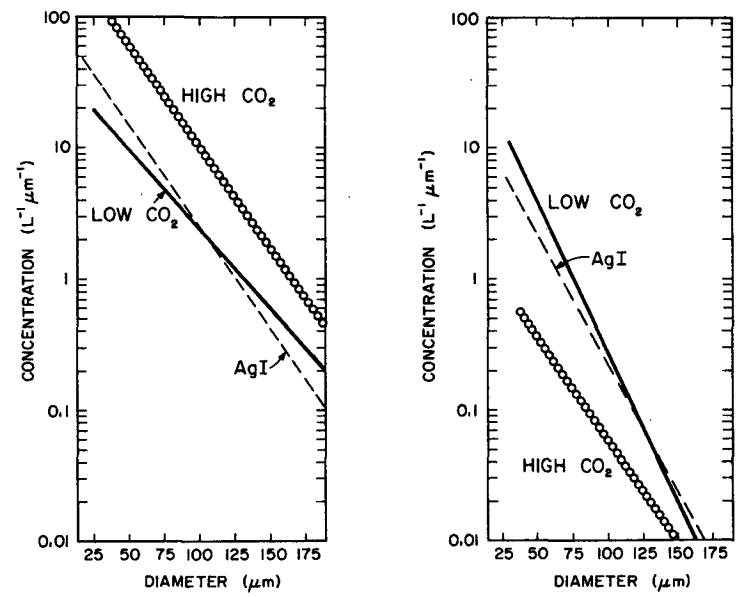

AGENT	TIME AFTER SEEDING (min)	CONC. (L^{-1})
LOW CO_2	3	525
AgI	3.5	1160
HIGH CO_2	3	3290

AGENT	TIME AFTER SEEDING (min)	CONC. (L^{-1})
LOW CO_2	37	195
AgI	38	110
HIGH CO_2	33	20

FIG. 16. 1D-C size spectra within the seeding plumes of the three clouds which were seeded on 21 March, 1979 for the two times indicated. The left diagram corresponds to seeding approximately 3 min after seeding and the diagram on the right corresponds to ~35 min after seeding. The observational temperatures ranged from −10 to −12°C.

Unauthenticated | Downloaded 04/22/24 12:27 AM UTC

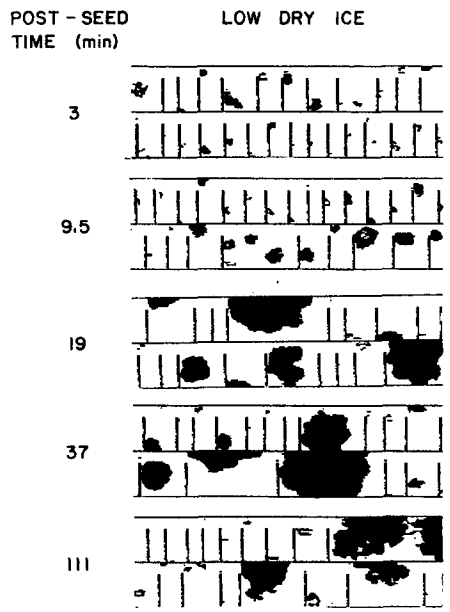

FIG. 17. Representative 2D-C images obtained at various times after seeding with low CO_2 rate on 21 March 1979. The maximum width of the probe corresponds to particle size of 800 μm.

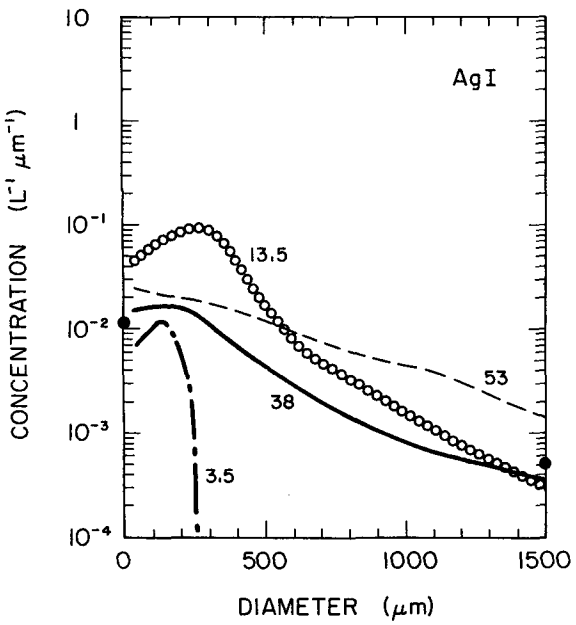

FIG. 19. Evolution of 2D-C size spectra after seeding with AgI on 21 March 1979. The number associated with each of the curves corresponds to the time after seeding at which the 2D-C size spectrum was calculated. The spectra are averages over the detectable plume width at that particular time.

was exponential. Third, the intercepts at 111 min from the low CO_2 case are indicated on Fig. 19 and they indicate that the slopes were very similar between the 111 min curve for the low CO_2 case and the 53 min curve for the AgI case. However, there were more particles in the cloud seeded with the AgI, since the intercepts were about a factor of 2.5 higher for that cloud. The AgI mode produced more and larger particles in a shorter time than did the low CO_2 rate.

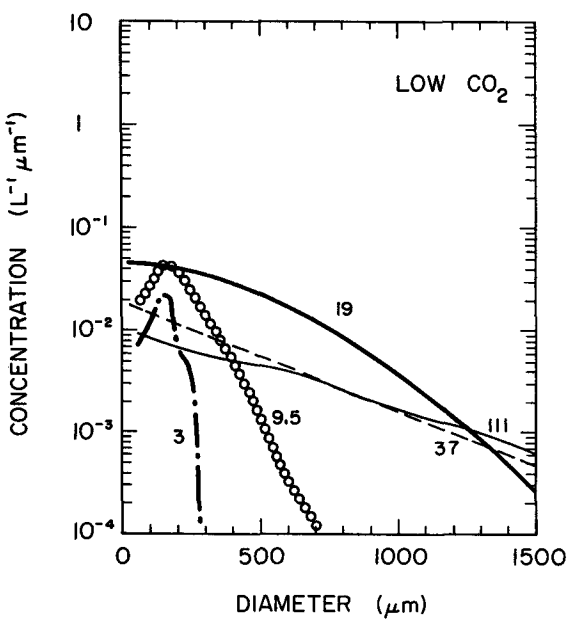

FIG. 18. Evolution of 2D size spectra after seeding with the low CO_2 rate on 21 March 1979. The numbers associated with each of the curves corresponds to the time after seeding at which the 2D-C size spectrum was calculated. The spectra are averages over the detectable plume width at that particular time.

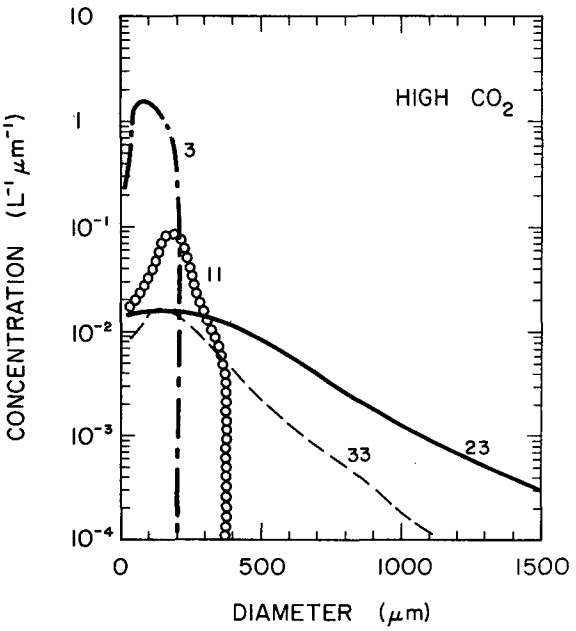

FIG. 20. Evolution of 2D-C size spectra after seeding with the high CO_2 rate on 21 March 1979. The number associated with each of the curves corresponds to the time after seeding at which the 2D-C spectrum was calculated. The spectra are averages over the detectable plume width at that particular time.

Unauthenticated | Downloaded 04/22/24 12:27 AM UTC

TABLE 1. Summary of concentrations on 21 and 18 March 1979.

Seeding method	Date	Time after seeding (min)	2D-C concentration (L^{-1})	Temperature (°C)
low CO_2	790321	3	3	−11
		9.5	9	−8
		19	22	−10
		37	6	−12
		111	5	−12
AgI	790321	3.5	2	−12
		13.5	33	−11
		38	7	−10
		53	16	−12
high CO_2	790321	3	119	−12
		11	11	−8
		23	9	−12
		33	4	−11
AgI	790318	9	9	−10
		18	38	−11
		24	36	−6
		61	8	−10
		145	13	−8

Fig. 20 shows the 2D-C spectra for the cloud seeded with the high CO_2 rate. First, there was a significantly slower size evolution with sizes increasing for only 23 min. Between 23 and 33 min the largest particles decreased from >1.5 to ~1 mm. Second, the peak in the size distribution, which may be attributable to the initial seeding event, was present through all the passes. Third, the concentration of ice crystals decreased at least an order of magnitude between 3 and 11 min, and this decrease continued for all penetrations.

Table 1 indicates the average 2D-C concentrations encountered within the seeded plumes. Peak concentrations of 22 L^{-1} (19 min after seeding) and 33 L^{-1} (13.5 min after seeding) were produced by seeding with low CO_2 and AgI, respectively. Concentrations declined after these times to 5 L^{-1} at 111 min after seeding with low CO_2 and to 16 L^{-1} at 53 min after seeding with AgI. 2D-C concentrations continually decreased in the cloud seeded with high CO_2 from 119 L^{-1} at 3 min to 4 L^{-1} at 33 min.

Spatial microphysical variations existed within the seeded plumes. This is elucidated in Fig. 21 which shows 2D-C size spectra as a function of position across a seeded plume. At 37 min after seeding with the low CO_2 rate and at a temperature of −12°C, the 2D-C spectra are plotted for three equal widths of the plume: east, center and west. The center region had the highest concentration of ice particles because of larger concentrations of small particles. There are a number of suggestions which could singularly or comparatively explain the illustrated difference between the center and the side regions. These possibilities include ice crystal multiplication processes operating differently in different regions, entrainment and sublimation effects on the edges or transport and diffusion acting on ice particles.

Fig. 22 shows the 1D-C size spectra diagram for the center, east and west sections of the plume discussed in association with Fig. 21. There were many more particles in the center region than on the

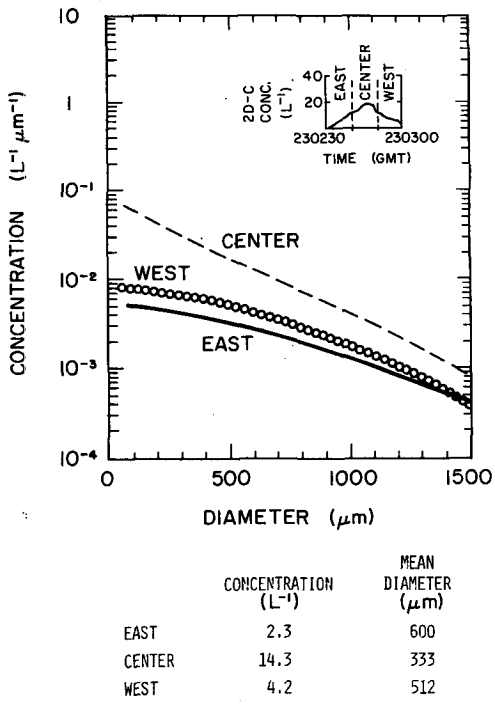

FIG. 21. 2D-C size spectra across a seeding plume on 21 March 1979. The three curves indicated are the distributions characteristic of the east, center and west portions of the plume at 37 min after seeding with the low CO_2 rate. The insert shows the manner in which the plume was partitioned.

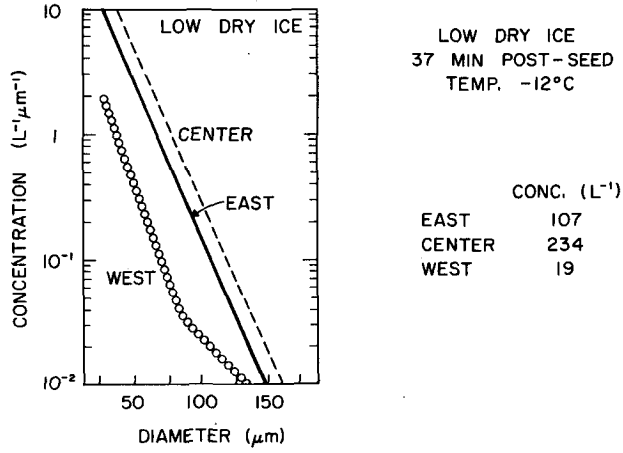

FIG. 22. 1D-C size spectra at 37 min after seeding with low CO_2 rate on 21 March 1979. The three curves on the diagram correspond to the east, center, and west edges of the cloud.

Unauthenticated | Downloaded 04/22/24 12:27 AM UTC

two sides. The slopes of all three were similar up to 75 μm, but for larger sizes, the center and east distributions continued to be exponential distributions, whereas the west edge curve became flatter. The reason for this is not known, but it may be related to the fact that the west edge was the upwind edge of the cloud.

Fig. 23 illustrates the evolution of the 2D-C size characteristics in the cloud seeded with AgI on 18 March. The maximum particle size generally increased with time. Distinct peaks in the concentration spectra did not occur on 18 March as opposed to the results from 21 March which showed peaks in the concentration profiles occurring at the small sizes soon after seeding. Between 61 and 145 min there was little difference between the 2D-C spectra, and from Table 1 and in rough agreement with the AgI seeding on 21 March, the largest average 2D-C concentrations occurred approximately 20 min after seeding and final average concentrations were near 15 L^{-1}.

Fig. 24 shows 2D-C size spectra obtained on 18 and 21 March when seeding was conducted with AgI. The curves correspond to times after seeding which were as close together as possible, essentially at 15 and 55 min. Both spectral slopes and intercepts at 15 min after seeding were similar, whereas only the spectral slopes at 55 min after seeding were similar. The two size spectra at 15 min overlapped at several sizes. For this latter time, many more particles were present on 21 March than on 18 March.

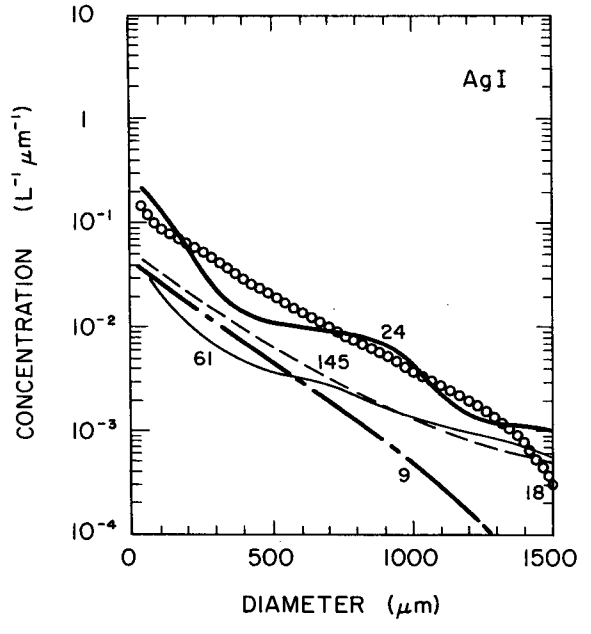

FIG. 23. 2D-C size spectra after seeding with AgI on 18 March 1979. The number associated with each of the curves corresponds to the time after seeding at which the 2D-C size spectrum was calculated. The spectra are averages over the detectable plume width at that particular time.

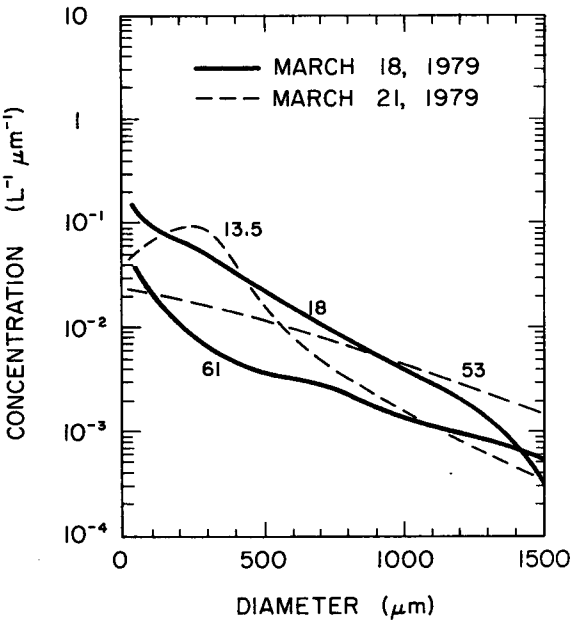

FIG. 24. 2D-C size spectra for AgI seeding on 18 March 1979 and on 21 March 1979. The solid lines correspond to results obtained on 18 March 1979 and the dotted lines correspond to results obtained on 21 March 1979. The times corresponding to the different curves are indicated by the numbers adjacent to those curves. The times after seeding for the two particular days were chosen to be as close together as possible for comparison purposes.

6. Concluding remarks

Observations made from seeding convective clouds with the low CO_2 rate and AgI have led to some speculation. It appears that after ~30 min, the seeding signatures from these two agents were similar. The clouds had been changed within this time from non-precipitating to continuously precipitating clouds. In the latter case, natural processes controlled precipitation production so these clouds may be termed "pseudo-natural" in that natural processes, instigated by seeding, were controlling precipitation production.

From this limited number of case studies, it is not possible to determine whether the low CO_2 rate or AgI is the most effective seeding agent for convective clouds over an orographic barrier. Both produce desirable seeding signatures and more case studies combined with placebos are necessary.

The high CO_2 rate of seeding clearly produced too many ice particles to develop a naturally precipitating cloud. How this overseeding killed the cloud is not known. Did the high concentration of ice crystals deplete the liquid water and then lower the water vapor pressure to saturation with respect to ice before any significant concentrations were

Unauthenticated | Downloaded 04/22/24 12:27 AM UTC

large enough to accrete and aggregate or did some unknown and unmeasured dynamical effect act to kill the cloud? Nevertheless, it is extremely significant that convective clouds can be prematurely dissipated by altering the microphysical structure of the clouds.

Acknowledgments. The authors wish to acknowledge the many contributions of the other participants in the SCPP and the assistance of our colleagues at the University of Wyoming. The guidance of Dr. Larry Vardiman, field director of the SCPP, was particularly effective, and the efforts of Dr. Donald Veal and Dr. Wayne Sand, pilot-scientists, were especially appreciated. This research was funded by the Department of Interior, Water and Power Resources Services, under Contract 7-07-83-V0001.

REFERENCES

Advisory Committee on Weather Control, 1957: Final Report, Vols. I and II. Washington, D.C.

Elliott, R. D., and W. A. Lang, 1967: Weather modification in the Southern Sierras. *J. Irrig. Drainage, Proc. ASCE*, **IR4,** 45–59.

Lamb, D., K. W. Nielsen, H. E. Klieforth and J. Hallett, 1976: Structure and of liquid water content in winter cloud systems over the Sierra Nevada. *J. Appl. Meteor.*, **15,** 763–775.

Mooney, M. L., and G. W. Lunn, 1968: The area of maximum effect resulting from the Lake Almandor randomized cloud seeding experiment. *J. Appl. Meteor.*, **8,** 68–74.

Reinking, R. F., 1975: Formation of graupel. *J. Appl Meteor.*, **14,** 745–754.

Weickmann, H. K., 1973: The modification of Great Lakes winter storms. NOAA Tech. Rep. ERL 265-APCL 26, 103 pp.

Unauthenticated | Downloaded 04/22/24 12:27 AM UTC